

Spectra for the Vacuum Cherenkov Effect in Astrophysical Electromagnetic Cascades with Lorentz Invariance Violation

Andrey Saveliev,^{a,b,*} Rafael Alves Batista^{c,d} and Feodor Mishin^e

^a*Immanuel Kant Baltic Federal University, Ul. A. Nevskogo 14, 236016 Kaliningrad, Russia*

^b*Lomonosov Moscow State University, GSP-1, Leninskiye Gory 1-52, 119234 Moscow, Russia*

^c*Sorbonne Université, Institut d'Astrophysique de Paris (IAP), CNRS UMR 7095, Paris, France*

^d*Sorbonne Université, Laboratoire de Physique Nucléaire et de Hautes Energies (LPNHE), Paris, France*

^e*Harrow School, Harrow, United Kingdom*

E-mail: anvsavelev@kantiana.ru

Lorentz invariance violation is a feature of several quantum gravity models in which Lorentz symmetry is broken at high energies, possibly leading to changes in particle behavior and interactions. In this work, we investigate vacuum Cherenkov radiation, a reaction in which an electron spontaneously emits a photon. This process, forbidden when Lorentz symmetry is unbroken, is a phenomenological consequence of some quantum gravity models. We derive, for the first time, the spectra for the vacuum Cherenkov reaction, and confirm our results numerically. These results can be used to derive limits on Lorentz invariance violation.

39th International Cosmic Ray Conference (ICRC2025)
15–24 July 2025
Geneva, Switzerland



ICRC 2025

The Astroparticle Physics Conference
Geneva July 15-24, 2025

*Speaker

1. Introduction

The Standard Model (SM) successfully describes electromagnetic, weak, and strong interactions but leaves key questions unanswered, such as the nature of dark matter and dark energy, the origin of neutrino masses, and the hierarchy problem, while also excluding gravity. Uniting the quantum field theory (QFT) of the SM with general relativity (GR) has led to the pursuit of a theory of quantum gravity (QG), which attempts to unify the SM and GR. These effects are presumed to become relevant at the Planck scale which is far beyond current experimental capabilities like those of the Large Hadron Collider. Nevertheless, certain QG effects might still be detectable through phenomena such as particle propagation on cosmic scales or frame-dependent energy shifts [1].

One potential signal of QG is Lorentz invariance violation (LIV). A common approach to study LIV within field theory is by extending the SM Lagrangian with additional terms, resulting in an effective field theory that captures possible deviations from Lorentz symmetry.

In terms of particle dynamics, phenomenologically, LIV primarily affects particle propagation by altering the dispersion relation, which then takes the form

$$E_{\text{LIV}}^2 = E_{\text{SM}}^2 + f_{\text{LIV}}(p), \quad (1)$$

where E_{LIV} is the energy of the particle in the presence of LIV, E_{SM} is its energy without LIV and $f_{\text{LIV}}(p)$ is the shift due to LIV, usually dominated by a single power of the particle's momentum p , i.e. $f_{\text{LIV}}(p) \propto \mathcal{O}(p^{n+2})$ with $n \geq 0$. This modification impacts the reaction thresholds [2, 3] and, consequently, alters the propagation length of particles.

By allowing Lorentz symmetry to be broken, LIV leads to a wealth of new processes that would otherwise be forbidden, such as spontaneous photon decay, photon splitting, vacuum Cherenkov (VC) radiation from charged particles, and even spontaneous disintegration of atomic nuclei. This ultimately impacts how particles travel in the universe.

In this work, we compute the spectra of photons resulting from VC radiation emitted during the propagation of high-energy electrons and positrons in astrophysical environments [4–6].

2. The kinematics of the vacuum Cherenkov effect

We consider modified dispersion relations that take the general form

$$E_e^2 = m_e^2 + p_e^2 + \sum_{n=0}^{\infty} \chi_n^e \frac{p_e^{n+2}}{M_{\text{Pl}}^n}, \quad E_\gamma^2 = k_\gamma^2 + \sum_{n=0}^{\infty} \chi_n^\gamma \frac{k_\gamma^{n+2}}{M_{\text{Pl}}^n}, \quad (2)$$

for electrons/positrons and photons, respectively. We closely follow the formalism from Ref. [7], restricting ourselves to the second-order case ($n = 2$), which features in a subset of the minimal [8] and non-minimal [9, 10] Standard-Model extension (SME).

For the formalism shown in Fig. 1 conservation of energy and momentum implies [7]

$$\frac{p_{\text{out},\perp}^2}{2p_{\text{in},e}x(1-x)} = \omega_{\text{LV}}^{\text{VC}}(x) \equiv -\frac{\chi_2^\gamma}{2} \frac{p_{\text{in},e}^3 x^3}{M_{\text{Pl}}^2} + \frac{\chi_2^e}{2} \frac{p_{\text{in},e}^3 (x^3 - 3x^2 + 3x)}{M_{\text{Pl}}^2}, \quad (3)$$

which can be promptly used to compute the VC differential rate $d\Gamma_{\text{VC}}/dx$ in terms of x [7],

$$\frac{d\Gamma_{\text{VC}}}{dx} = \alpha \left(\frac{2}{x} - 2 + x \right) \omega_{\text{LV}}^{\text{VC}}(x), \quad (4)$$

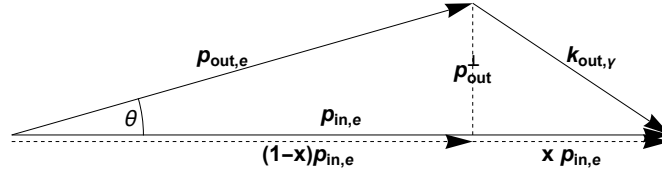


Figure 1: VC kinetics formalism used in [7] and in the present work for the momenta of the incoming electron, outgoing photon and outgoing electron labeled $p_{in,e}$, $k_{out,\gamma}$ and $p_{out,e}$, respectively.

with α being the fine-structure constant.

3. Probabilities and Rates for the Vacuum Cherenkov Effect

This work is part of a larger ongoing program aiming to perform detailed Monte Carlo simulations of electromagnetic cascades considering LIV. For this reason, we compute the detailed spectrum of the emitted photons, whose total emission rate (Γ_{VC}) can be written as¹:

$$\Gamma_{VC} = \begin{cases} \Gamma_1 \equiv \alpha \mathcal{G}_0 \frac{p_{in,e}^3}{M_{Pl}^2}, & x \in (0; 1), (\chi_2^e \geq 0) \wedge (\chi_2^\gamma \leq \chi_2^e), \\ \Gamma_2 \equiv \alpha \mathcal{G}_+ \frac{p_{in,e}^3}{M_{Pl}^2}, & x \in (0; x_{VC,+}), 0 < \chi_2^e < \chi_2^\gamma, \\ \Gamma_3 \equiv \alpha (\mathcal{G}_0 - \mathcal{G}_-) \frac{p_{in,e}^3}{M_{Pl}^2}, & x \in (x_{VC,+}; 1), \chi_2^\gamma < \chi_2^e < 0, \\ [\text{no VC}], & \text{else} \end{cases} \quad (5)$$

where

$$x_{VC,\pm} = -\frac{3\chi_2^e}{2(\chi_2^\gamma - \chi_2^e)} \pm \frac{\sqrt{3\chi_2^e(4\chi_2^\gamma - \chi_2^e)}}{2|\chi_2^\gamma - \chi_2^e|}. \quad (6)$$

A final point to be considered concerns the kinematical threshold for the reaction; VC is only possible if the momentum of the incoming electron exceeds a threshold value $p_{VC,thr}$, i.e. $p_{in,e} > p_{VC,thr}$. For the case considered here, LIV of order $n = 2$, the only non-zero coefficients are χ_2^e and χ_2^γ . In this case the threshold values may be found in Ref. [2].

The existence of a (lower) threshold, together with the integration limits for x , may be used in specific cases to determine the momenta ($k_{out,\gamma}$ and $p_{out,e}$) of the outgoing particles.

With these results we now can calculate the total interaction rate for VC, Γ_{VC} , by integrating

¹For a full derivation, the reader is referred to Ref. [11].

Eq. (4) in the range specified in Eq. (7), for a given combination of χ_2^e and χ_2^γ , obtaining

$$\Gamma_{\text{VC}} = \begin{cases} \Gamma_1 \equiv \alpha \mathcal{G}_0 \frac{p_{\text{in},e}^3}{M_{\text{Pl}}^2}, & x \in (0; 1), (\chi_2^e \geq 0) \wedge (\chi_2^\gamma \leq \chi_2^e), \\ \Gamma_2 \equiv \alpha \mathcal{G}_+ \frac{p_{\text{in},e}^3}{M_{\text{Pl}}^2}, & x \in (0; x_{\text{VC},+}), 0 < \chi_2^e < \chi_2^\gamma, \\ \Gamma_3 \equiv \alpha (\mathcal{G}_0 - \mathcal{G}_-) \frac{p_{\text{in},e}^3}{M_{\text{Pl}}^2}, & x \in (x_{\text{VC},+}; 1), \chi_2^\gamma < \chi_2^e < 0, \\ [\text{no VC}], & \text{else} \end{cases} \quad (7)$$

where

$$x_{\text{VC},\pm} = -\frac{3\chi_2^e}{2(\chi_2^\gamma - \chi_2^e)} \pm \frac{\sqrt{3\chi_2^e(4\chi_2^\gamma - \chi_2^e)}}{2|\chi_2^\gamma - \chi_2^e|}, \quad (8)$$

and the parameters \mathcal{G}_\pm are defined as

$$\mathcal{G}_\pm \equiv \left[37(\pm S - 6\chi_2^\gamma)\chi_2^e\chi_2^\gamma - 64(\chi_2^e)^3 - (\pm 14S - 207\chi_2^\gamma)(\chi_2^e)^2 - 10(\pm 5S - 16\chi_2^\gamma)(\chi_2^\gamma)^2 \right] \\ \times \frac{\chi_2^e(\pm S - 3\chi_2^e)}{160(\chi_2^\gamma - \chi_2^e)^4}, \quad \text{and} \quad \mathcal{G}_0 \equiv \frac{157\chi_2^e - 22\chi_2^\gamma}{120}, \quad (9)$$

wherein $S \equiv \sqrt{3\chi_2^e(4\chi_2^\gamma - \chi_2^e)}$. Employing these definitions, we can now understand the behavior of the VC rate considering the χ_2^e - χ_2^γ parameter space. The possible values of Γ_{VC} for all the different parameter combinations presented in Eq. (7).

From Eq. (7) we can finally calculate the differential probability (dP_{VC}/dx) with respect to the fraction x of momentum carried away by the photon, which together with the threshold values gives

$$\frac{dP_{\text{VC}}}{dx} = \max \left\{ 0, \alpha \left(\frac{2}{x} - 2 + x \right) \frac{\omega_{\text{LV}}^{\text{VC}}(x)}{\Gamma_{\text{VC}}} \right\}, \quad (10)$$

for $p_{\text{in},e} > p_{\text{VC,thr}}$ with Γ_{VC} given by Eq. (7).

Based on the symmetry of the allowed values of x , cf. (7), we illustrate Eq. (10) by exemplarily considering parameter combinations which obey the relation $|\chi_2^\gamma \chi_2^e| = 10^{-10}$.

4. Results

We present the VC spectra for incoming electrons with initial energy $E_{\text{in},e} = 10^{21}$ eV, exploring various combinations of LIV parameters. For each scenario, we generate 10^6 random samples following Eq. (10). These simulations account for the full VC cascade, i.e. the repeated VC-induced photon emission until the electron energy drops below the VC threshold.

The emission of VC photons is treated as instantaneous, as the associated emission rate (Γ_{VC}) implies distances much shorter than all other relevant processes acting on galactic and cosmological scales. Additionally, we employ the co-linear approximation, wherein the emitted particles are parallel to their parent – a good approximation for high-energy particles.

We identify four distinct parameter combinations, each corresponding to qualitatively different emission spectra. We refer to them as cases A–D, defined as follows:

$$\text{A} : \chi_2^\gamma < \chi_2^e < 0, \quad \text{B} : \chi_2^\gamma < 0 \leq \chi_2^e, \quad \text{C} : 0 < \chi_2^\gamma \leq \chi_2^e, \quad \text{D} : 0 < \chi_2^e < \chi_2^\gamma. \quad (11)$$

An important finding emerging directly from Fig. 3 is the appearance of a lower-energy cut-off in the spectrum of one of the outgoing particles, depending on the parameter regime. This is evident for the electron spectra corresponding to LIV parameters within range D, and in the photon spectra for parameters within range A.

This behaviour can be understood by examining the integration limits. For $x \in (0, x_{\text{VC},+})$, corresponding to the condition $0 < \chi_2^e < \chi_2^\gamma$ as defined in Eq. (7), we have $x < x_{\text{VC},+}$, implying $1 - x > 1 - x_{\text{VC},+}$. Since the minimum incoming electron momentum is set by the VC threshold ($p_{\text{VC},\text{thr}}$), the outgoing electron momentum satisfies $p_{\text{VC},\text{min}} \leq p_{\text{out},e} \leq p_{\text{VC},\text{thr}}$ for $0 < \chi_2^e < \chi_2^\gamma$, where $p_{\text{VC},\text{min}}$ is defined as $p_{\text{VC},\text{min}} \equiv (1 - x_{\text{VC},+})p_{\text{VC},\text{thr}}$. Conversely, for the integration limits $x \in (x_{\text{VC},+}; 1)$, corresponding to $\chi_2^e < \chi_2^\gamma < 0$, we have $x \geq x_{\text{VC},+}$ and hence $1 - x < 1 - x_{\text{VC},+}$. This same reasoning also implies that $k_{\text{out},\gamma} \geq k_{\text{VC},\text{min}}$ for $\chi_2^e < \chi_2^\gamma < 0$, where $k_{\text{VC},\text{min}}$ is defined as $k_{\text{VC},\text{min}} \equiv x_{\text{VC},+}p_{\text{VC},\text{thr}}$.

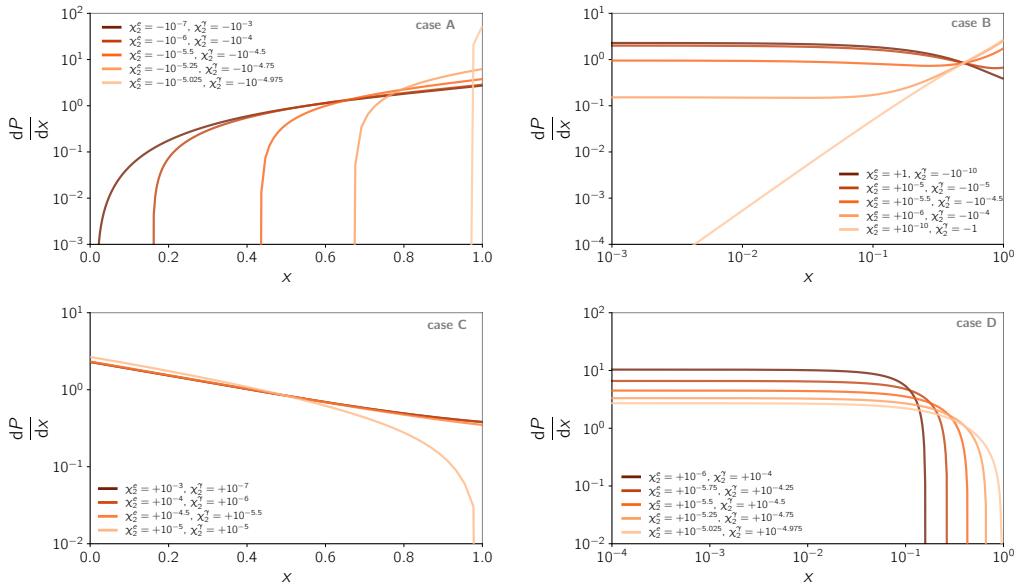


Figure 2: Differential probability distribution ($\frac{dP_{\text{VC}}}{dx}$) for various combinations of χ_2^e and χ_2^γ , with $|\chi_2^\gamma \chi_2^e| = 10^{-10}$. Each panel corresponds to different regimes, based on the signs of χ_2^γ and χ_2^e , according to Eq. (11)

Another prominent feature common to all photon spectra is that all of them follow a particular power law, extending from the VC threshold up to nearly the initial electron energy (see Fig.3). This arises because the differential emission probability is independent of the incoming electron momentum, as given in Eq.(10).

We now turn to the different cases of the photon spectra, starting with a feature common to the cases C and D. While for higher energies one can see the power-law behavior $dN/dE_{\text{out},\gamma}$ of proportional to $E_{\text{out},\gamma}^{-1}$ as described above, the spectrum flattens to $dN/dE_{\text{out},\gamma} \propto E_{\text{out},\gamma}^0$ for lower

energies. This is an immediate consequence of the differential probability distribution (see Eq. (10)) being peaked around zero and then falling roughly linearly for higher values of x , as shown in the corresponding panels of Fig. 2. The transition between these two regimes is determined by the VC threshold value.

The photon spectra for case A exhibits a lower cut-off and, for χ_2^γ and χ_2^e being close to each other, a gap near the initial momentum, which widens as the two values converge. This gap-like feature is once more a direct consequence of the corresponding differential probability distributions (cf. Fig. 2). Here we can see that the closer the two values are to each other the narrower the differential distribution, which peaks around 1, becomes, producing a narrow peak in the photon spectrum close to the initial momentum value and then another peak before the electron drops below the threshold value. Once the values get further apart, the distribution widens, which itself results in a widening of the peak as well as its shift to lower momentum values.

Finally, for case B there are two different regimes for $dN/dE_{\text{out},\gamma}$ at lower momentum values of the outgoing photons – either a quadratic increase for $|\chi_2^\gamma| \gg \chi_2^e$ or a flat spectrum for $|\chi_2^\gamma| \ll \chi_2^e$. This behavior may again be explained by analyzing the corresponding plots in Fig. 2. Both regimes correspond directly to the behavior of the corresponding differential probability densities, as due to the fact that they are independent of the momentum of the incoming electron, the spectrum is effectively a superposition of many of such individual distributions.

Proceeding to the electron spectra, for case A we see that the spectral shape of $dN/dE_{\text{out},e}$ is a flat spectrum with a sharp cut-off which occurs when the electron momentum drops below the VC threshold value. The only spectral variation appears right below the cut-off where the spectrum either slightly rises or falls. This is, again, a direct consequence of the corresponding differential probability distribution function, but this time resulting in a reverse relationship compared to the photon spectra which is due to the fact that the electron carries away the remaining fraction of the incoming momentum, $1 - x$.

The other case for which the electron spectrum displays some interesting features (apart from the lower cut-off described above) is for LIV parameter values lying within the ranges denoted as case D. If χ_2^e and χ_2^γ are fairly apart from each other, one gets an almost monochromatic emission due to the differential probability shown in the top panel of Fig. 2. We can see that for electrons it is tightly peaked around 1, which translates into the monochromatic spectrum. By further emitting photons, this distribution simply moves to lower momentum values until it reaches the threshold value at which point it does not change anymore. Once the values of χ_2^e and χ_2^γ are getting close to each other, this nearly monochromatic spectrum acquires a low-momentum tail, again simply resulting directly from the now wider differential probability distribution.

5. Discussion and Outlook

In this work, we investigated if the vacuum Cherenkov leaves a discernible imprint in high-energy gamma-ray data. We found that in regions like the Milky Way, where magnetic fields are modest (~ 0.1 nT), that VC dominates over synchrotron losses by several orders of magnitude. This is not true in the surroundings of highly magnetized compact objects, where strong magnetic fields incur synchrotron losses that depend quadratically on the field. However, the radiated synchrotron power when Lorentz symmetry is broken may not follow trivially.

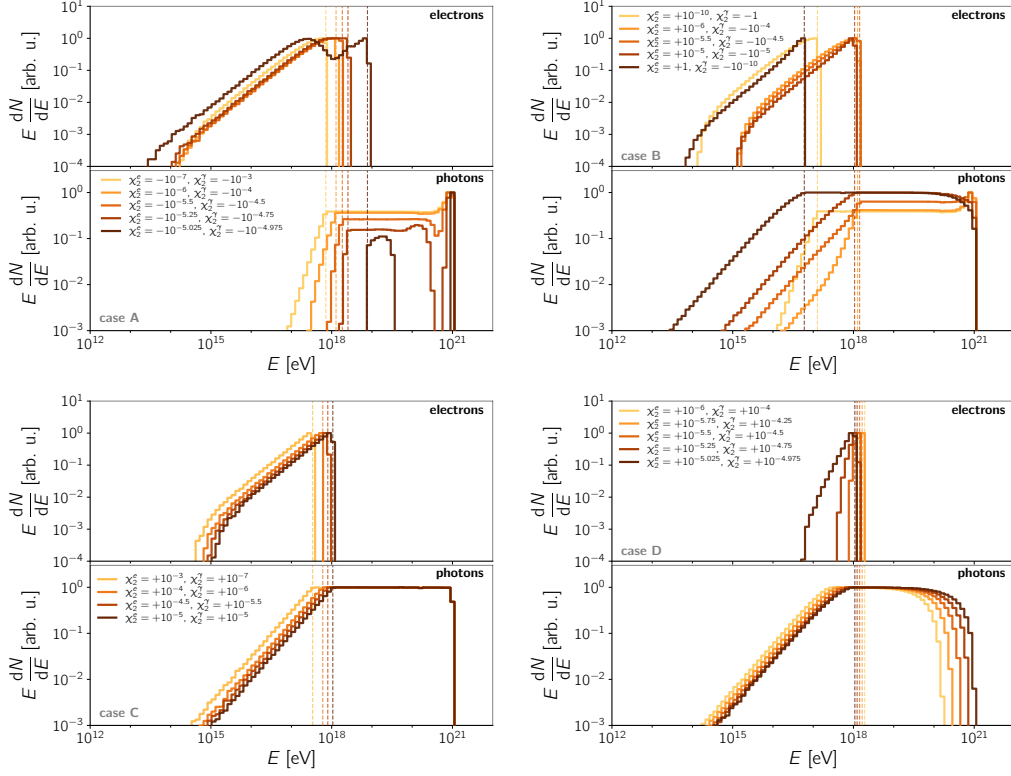


Figure 3: Results of Monte Carlo simulations for various χ_2^e and χ_2^γ combinations. Dashed lines refer to the corresponding threshold energies. Spectra are energy-weighted to highlight the $dN/dE \propto E^{-1}$ behaviour. The normalization of the distributions is arbitrary.

Compared to inverse Compton scattering of energetic electrons off photon backgrounds such as the cosmic microwave background (CMB) and the extragalactic background light (EBL), VC is also more efficient.

While our primary focus was on electrons and positrons, our finding can be immediately extended to other charged leptons, namely muons and taus, provided that their lifetime exceeds the VC time scale.

A noteworthy feature of our framework is that we allow the Lorentz-violating coefficients to differ by particle species. Because charge, parity, and time (CPT)-odd terms flip the signs between particles and antiparticles, this distinction is indispensable for any realistic phenomenology.

For simplicity, we based our analysis on direction-independent LIV terms and worked in a preferred frame. While this makes simulations more manageable, it inevitably masks possible anisotropic signatures that could, in principle, be observed.

We presented the first complete derivation of the vacuum Cherenkov radiation spectrum based on the interaction rates from [7]. We find that the commonly used “binary” approach – assuming the electron drops to the VC threshold and the photon carries away the momentum difference – is generally inaccurate. While outgoing electrons can be nearly monochromatic in some cases (see Fig. 3), the photon spectrum is typically broader, requiring a full treatment of the VC process including successive energy losses.

Due to the short interaction time, VC radiation occurs almost instantly after electron creation, making the resulting spectra valuable inputs for modeling electromagnetic cascades over Galactic and larger scales. As part of a larger-term plan [12], we plan to integrate this feature into the CRPropa framework [13–15], extending our previous work [16].

Future studies will also explore how LIV affects other key processes like inverse Compton scattering, pair production, and photon decay. In particular, scenarios where both VC radiation and photon decay are allowed by specific values of χ_2^e and χ_2^γ merit deeper investigation.

Acknowledgments

RAB acknowledges the support of the Agence Nationale de la Recherche (ANR), project ANR-23-CPJ1-0103-01.

References

- [1] A. Addazi et al., *Prog. Part. Nucl. Phys.* **125** (2022) 103948 [2111.05659].
- [2] T. Jacobson et al., *Phys. Rev. D* **67** (2003) 124011 [hep-ph/0209264].
- [3] A. Saveliev et al., *J. Cosmol. Astropart. Phys.* **2011** (2011) 046 [1101.2903].
- [4] C. Kaufhold et al., *Nucl. Phys. B* **734** (2006) 1 [hep-th/0508074].
- [5] D. Anselmi et al., *Phys. Rev. D* **83** (2011) 056010 [1101.2019].
- [6] M. Schreck, *Phys. Rev. D* **96** (2017) 095026 [1702.03171].
- [7] G. Rubtsov et al., *Phys. Rev. D* **86** (2012) 085012 [1204.5782].
- [8] D. Colladay et al., *Phys. Rev. D* **58** (1998) 116002 [hep-ph/9809521].
- [9] V.A. Kostelecký et al., *Phys. Rev. D* **80** (2009) 015020 [0905.0031].
- [10] A. Kostelecký et al., *Phys. Rev. D* **88** (2013) 096006 [1308.4973].
- [11] A. Saveliev et al., *Phys. Rev. D* **111** (2025) 083001 [2412.17514].
- [12] R. Alves Batista et al., *Class. Quant. Grav.* **42** (2025) 032001 [2312.00409].
- [13] R. Alves Batista et al., *J. Cosmol. Astropart. Phys.* **5** (2016) 038 [1603.07142].
- [14] R. Alves Batista et al., *J. Cosmol. Astropart. Phys.* **09** (2022) 035 [2208.00107].
- [15] S. Aerdker et al., *Proc. of Science ICRC2025* (2025) 964.
- [16] A. Saveliev et al., *Class. Quant. Grav.* **41** (2024) 115011 [2312.10803].